Quantum mechanical study of resonant scattering in a nuclear Λ scheme

S. Gheysen and J. Odeurs
Instituut voor Kern-en Stralingsfysica, K.U.Leuven, Celestijnenlaan 200D, B-3001 Leuven, Belgium
(Received 5 September 2006; published 31 October 2006)

We present a fully quantum mechanical treatment of resonant scattering of gamma radiation in a nuclear medium exhibiting a Λ scheme through level mixing. A framework is presented to derive the radiation intensity for N effective scatterers contributions. A closed-form solution for the radiation intensity is obtained and compared to the generic expression of EIT in an atomic Λ scheme. Although the nuclear scheme does not fulfill EIT conditions, the observable effects are similar. We show that the change in polarization of the scattered radiation, due to the level mixing, gives rise to the development of a strong complementary polarization state which is *delayed* with respect to the incident photon to a reduction in absorption because this state does not interfere with the incident photon.

DOI: 10.1103/PhysRevB.74.155443 PACS number(s): 76.80.+y, 42.25.Bs, 42.50.Gy

I. INTRODUCTION

Resonant scattering in a three-level Λ scheme is an intensively investigated topic in the field of quantum optics. Such a system is closely related to the phenomenon of electromagnetically induced transparency (EIT). The phenomenon of EIT can be realized in a two-field Λ scheme and basically implies that an atom becomes transparent for a resonant, probe field under the influence of a second field, the so-called driving field, see Ref. 1 for an overview.

Recently, the first observation of EIT for *gamma* radiation has been reported.[2] However, it has been pointed out[3] that, in order to observe EIT as known in quantum optics, the two lower lying states must be metastable, which is not the case in the nuclear Λ scheme[4] from Ref. 2. In this paper we want to approach the induced transparency of gamma photons from a theoretical point of view in order to explain why a partial transparency of gamma photons is observed, despite the condition of excited states with similar decay rates. Moreover, we predict an appreciable time delay of the scattered photon field.

The importance of this transparency for gamma photons is not merely the extension of the range of wavelengths where EIT is observed. Its main impact concerns the true *single particle* nature in these experiments, whereas previous work almost always dealt with large numbers of (coherent) photons. The nuclear source, consisting of an ensemble of excited nuclei, emits individual gamma photons in a stochastic way. The different gamma photons do not have any phase relation among them. Moreover, due to their high energy (>10 keV), their individual detection is straightforward.

Although the semiclassical optical model, originally developed by Hamermesh,[5] is widely used when dealing with nuclear resonant scattering, we opt for the coherent path model, based on the work of Heitler[6] and Harris[7] and recently updated by Hoy.[8] Moreover, this fully quantum mechanical model has been very successful in describing a resonant Mössbauer detector[9] and has provided interpretation of the gamma echo.[10] It has also added some insight in the phenomena of speed-up and dynamical beats present in nuclear resonant forward scattering of synchrotron radiation.[11]

This coherent path model seems to be the most natural choice of description since we are dealing with single photons in interaction with an ensemble of nuclei. In an appendix, we also justify the use of a single photon wave function in this model as emerging from the photodetection process.

In Sec. II, a theoretical framework is built starting from first principles. Eventually, a closed-form solution for the photon wave function is derived. Some selected cases are discussed in Sec. III, where emphasis is given to the comparison of the nuclear level mixing scheme with a typical atomic Λ scheme. Both the frequency and time domain picture are presented. Finally, the main conclusions are summarized in Sec. IV.

II. COHERENT PATH APPROACH

A. Model outline

First, we present a brief, but general description of the model. We start from the time-dependent Schrödinger equation. The Hamiltonian of the system can be written as the sum of two parts: H_0 describes the unperturbed nuclei and the free radiation field (if present), while V is the interaction Hamiltonian that describes the transitions between the nuclear levels induced by the radiation field(s). The actual state of the system is given by

$$|\Psi(t)\rangle = \sum_n c_n(t) e^{-iE_n t/\hbar} |\phi_n\rangle \tag{1}$$

with $|\phi_n\rangle$ an eigenstate of H_0 and $E_n = \hbar\omega_n$ its corresponding energy. The coefficients $c_n(t)$ must satisfy the Schrödinger equation, which leads to a set of coupled differential equations

$$i\hbar \frac{dc_n(t)}{dt} = \sum_m c_m(t) e^{i(\omega_n - \omega_m)t} \langle \phi_n | V | \phi_m \rangle + i\hbar \delta_{1n} \delta(t), \tag{2}$$

where δ_{1n} is the Kronecker delta and $\delta(t)$ the Dirac delta function. The inhomogeneous term is added for the following reasons. First, the solution must satisfy the initial condition that the system is in a well-defined state, e.g., $c_n(0) = \delta_{1n}$. Second, although we choose a solution that only in-

volves positive times, it will be extended to the negative time axis for analytical reasons. All amplitudes $c_n(t)$ are chosen such that $c_n(t<0)=0$. Following Heitler[6] the discontinuity in $c_1(t)$ arising at $t=0$ is correctly dealt with by addition of the inhomogeneous term. In practice, in a time-differential coincidence measurement,[12] $t=0$ can be defined by the detection of precursor radiation, which precedes the gamma radiation of interest. It is more interesting, however, to use the Fourier transform of Eq. (2). If we apply

$$c_n(t) = -\frac{1}{2\pi i}\int_{-\infty}^{\infty} d\omega C_n(\omega) e^{i(\omega_n-\omega)t}, \tag{3}$$

then Eq. (2) can be rewritten as

$$(\omega - \omega_n + i\epsilon)C_n(\omega) = \sum_m C_m(\omega)\frac{V_{nm}}{\hbar} + \delta_{n1} \tag{4}$$

with $V_{nm} \equiv \langle \phi_n | V | \phi_m \rangle$ a time-independent matrix element describing a transition from the mth to the nth eigenstate of H_0. The introduction of $+i\epsilon(\epsilon>0)$ ensures the proper causality relations.[6] This term eventually disappears from any physical result by considering the limit $\epsilon \to 0^+$.

The eigenstates of H_0 are given by the direct product of an ensemble of unperturbed nuclear states and the states of the free radiation field: $|\phi_n\rangle = |\text{nuclei}\rangle \otimes |\text{field}\rangle$. In the case of a Mössbauer scheme the nuclear ensemble consists of one source nucleus (S) and N absorber nuclei (A) while the radiation field can be expressed as a photon number state (P): $|\phi_n\rangle = |S\rangle|A_1\rangle|A_2\rangle \cdots |A_N\rangle|P\rangle$. The number of $|\phi_n\rangle$ states is limited by a proper choice of the initial state as will be clear later on.

B. Three-level system

To relate to a real situation, we consider the case of ^{57}Fe nuclei embedded in a $FeCO_3$ single crystal. Below the Néel temperature [$T_N=38.3(3)$ K (Ref. 13)] the nuclei experience a strong axial electric field gradient (efg) and a magnetic hyperfine field, which is essentially parallel to the axis defined by the efg. The combination of these hyperfine interactions gives rise to an accidental level crossing. At the temperature of $T=30.5(5)$ K, the $|m_e=1/2\rangle \equiv |2\rangle$ and $|m_e=-3/2\rangle \equiv |3\rangle$ levels are crossing,[4] where m_e is the magnetic quantum number of a sublevel of the $I=3/2$ nuclear excited state. The energies of the excited states with respect to the $|m_g=-1/2\rangle \equiv |1\rangle$ ground state are $\hbar\omega_2$ and $\hbar\omega_3$, respectively. For the sake of simplicity we are limiting the model to the levels that are involved in the resonant scattering at the level crossing, i.e., the transition from the $|1\rangle$ ground state to the $|2\rangle$ and $|3\rangle$ excited states, as visualized in Fig. 1.

If the source photons are incident parallel to the crystal symmetry axis, which coincides with the principal axis of the efg, then the interaction Hamiltonian can be written as

$$V = V_+|2\rangle\langle 1| + V_-|3\rangle\langle 1| + \hbar\Omega|2\rangle\langle 3| + \text{H.c.} \tag{5}$$

The 14.4 keV gamma transition in ^{57}Fe is essentially an $M1$ magnetic dipole transition. Hence, the first term describes the interaction of the radiation with the nucleus in the magnetic dipole approximation, with $V_+=\langle 2|\mathcal{H}^+|1\rangle$ and $V_-=\langle 3|\mathcal{H}^+|1\rangle$, with $\mathcal{H}^\pm$ the magnetic dipole operator in the case of a σ^+ (σ^-) polarized (electro)magnetic field. Explicit expressions for these matrix elements can be found in Ref. 14. They are basically proportional to the product of a Wigner rotation matrix element and a Clebsch-Gordan coefficient. It is also assumed that a mixing interaction Ω between the excited states is present. As the crossing levels are degenerate in energy, they are very sensitive to small nonaxial fields that can induce transitions between them. For more details on this mixing interaction we refer to Ref. 4. This three-level system is summarized in Fig. 1.

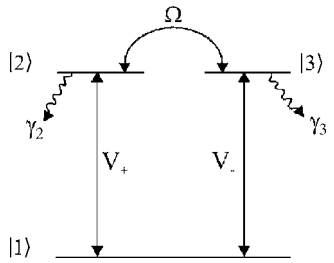

FIG. 1. Schematical representation of the three-level system under consideration. The two excited states $|2\rangle$ and $|3\rangle$ are mixed by an interaction Ω and couple to the ground state through V_+ and V_-, respectively.

In Mössbauer spectroscopy[15] a radioactive source is used as the initial source of gamma photons. The photons are emitted one by one, in a statistical and uncorrelated manner. If we adopt a circular basis for their description, then one can say that, as the source is unpolarized, one-half of the emitted photons are left circularly polarized (σ^-) and the other half is right circularly polarized (σ^+). This means that we can treat their contribution independently. We restrict the model to σ^+ source photons and keep in mind that the treatment of σ^- source photons can be done analogously. Due to the breaking of the axial symmetry by the level mixing, however, a σ^+ source photon can be absorbed while a σ^- photon is reemitted. Therefore, as soon as the first scattering takes place, we must take into account two photon fields. Because these two fields have mutual perpendicular polarizations, the total radiation intensity will be just the sum of both field intensities.

The absorber is treated as a collection of N identical nuclei, which effectively scatter the gamma photon. The number of scattering centers N is shown to be proportional to the more common effective optical thickness β,[8]

$$N = \frac{\beta\gamma}{2f\gamma_r} \tag{6}$$

with γ the total decay rate of the nuclear excited state, γ_r the radiative decay rate and f the recoilless fraction. In a multilevel nucleus, however, the effective thickness is reduced according to[16]

$$\beta \to \frac{1}{2I_g+1}\frac{2L+1}{2I_e+1}\beta \tag{7}$$

with $I_{g/e}$ the spins of the nuclear ground and excited states and L the multipolarity of the radiation (here $L=1$).

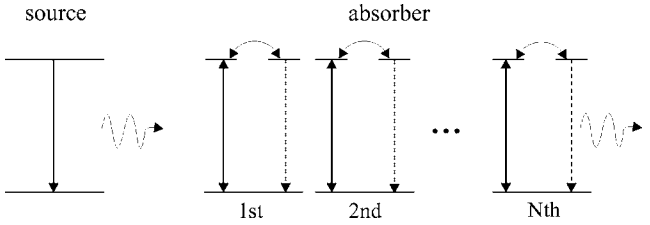

FIG. 2. Physical model of nuclear resonant scattering in a three-level scheme. The horizontal lines present the unperturbed nuclear eigenstates and the arrows indicate the interactions.

A schematical overview of the physical system under consideration is given in Fig. 2. A single-line source nucleus decays and emits a σ^+ (or σ^-) photon. This photon is scattered by N absorber nuclei. In this process the photon can retain its initial polarization (solid line) or it can change its polarization through the mixing interaction (dashed line).

C. General equations

If we apply the above mathematical formalism to the system of a source nucleus and N resonant absorber nuclei, located between the source and the detector, then five structurally distinct eigenstates of H_0 and their corresponding amplitudes can be identified:

(i) $|\phi_1\rangle \equiv |S\rangle = |S^e, A_m^1, 0_{\mathbf{k},\sigma^+}, 0_{\mathbf{k}',\sigma^-}\rangle$ with $S(\omega)$ the amplitude corresponding to the source nucleus in the excited state ($\hbar\omega_s$), the absorber nuclei in the ground state and no photons present. $|S\rangle$ is the initial state in the model considered.

(ii) $|\phi_2\rangle \equiv |P_{\mathbf{k}}^+\rangle = |S^g, A_m^1, 1_{\mathbf{k},\sigma^+}, 0_{\mathbf{k}',\sigma^-}\rangle$ with $P_{\mathbf{k}}^+(\omega)$ the amplitude corresponding to the source nucleus in the ground state, the absorber nuclei in the ground state and one photon with wave number $\mathbf{k}$, σ^+ polarization and energy $\hbar\omega_k$.

(iii) $|\phi_3\rangle \equiv |P_{\mathbf{k}'}^-\rangle = |S^g, A_m^1, 0_{\mathbf{k},\sigma^+}, 1_{\mathbf{k}',\sigma^-}\rangle$ with $P_{\mathbf{k}'}^-(\omega)$ the amplitude corresponding to the source nucleus in the ground state, the absorber nuclei in the ground state and one photon with wave number $\mathbf{k}'$, σ^- polarization and energy $\hbar\omega_{k'}$.

(iv) $|\phi_4\rangle \equiv |A_m\rangle = |S^g, A_m^2, 0_{\mathbf{k},\sigma^+}, 0_{\mathbf{k}',\sigma^-}\rangle$ with $A_m(\omega)$ the amplitude corresponding to the absorber nucleus m at position $\mathbf{x_m}$ in the excited state $|2\rangle$ ($\hbar\omega_2$), all other nuclei in the ground state and no photons present.

(v) $|\phi_5\rangle \equiv |B_m\rangle = |S^g, A_m^3, 0_{\mathbf{k},\sigma^+}, 0_{\mathbf{k}',\sigma^-}\rangle$ with $B_m(\omega)$ the amplitude corresponding to the absorber nucleus m at position $\mathbf{x_m}$ in the excited state $|3\rangle$ ($\hbar\omega_3$), all other nuclei in the ground state and no photons present.

It must be noted that this model considers one particular value of $\mathbf{k}$ (and $\mathbf{k}'$), which can be seen as a plane wave approximation. However, at the end of the derivation, a realistic wave packet is reconstructed as the (infinite) sum of these plane wave solutions.

Here, decay processes due to electron conversion are not explicitly taken into account. It can be easily shown, however, that their contribution is limited to an additional term γ_c in the total decay rate $\gamma = \gamma_r + \gamma_c$.[9]

If we assume that at $t=0$ only the source nucleus, at the origin, is excited, or $|\Psi(t=0)\rangle = |S\rangle$, the following set of coupled linear equations from Eq. (4) are obtained:

$$(\omega - \omega_s + i\epsilon)S(\omega) = 1 + \sum_{\mathbf{k}} P_{\mathbf{k}}^+(\omega)\frac{V_{SP_{\mathbf{k}}}}{\hbar}, \tag{8}$$

$$(\omega - \omega_k + i\epsilon)P_{\mathbf{k}}^+(\omega) = S(\omega)\frac{V_{P_{\mathbf{k}}S}}{\hbar} + \sum_m A_m(\omega)\frac{V_{P_{\mathbf{k}}A}}{\hbar}e^{-i\mathbf{k}\cdot\mathbf{x_m}}, \tag{9}$$

$$(\omega - \omega_{k'} + i\epsilon)P_{\mathbf{k}'}^-(\omega) = \sum_m B_m(\omega)\frac{V_{P_{\mathbf{k}'}B}}{\hbar}e^{-i\mathbf{k}'\cdot\mathbf{x_m}}, \tag{10}$$

$$(\omega - \omega_2 + i\epsilon)A_m(\omega) = \sum_{\mathbf{k}} P_{\mathbf{k}}^+(\omega)\frac{V_{AP_{\mathbf{k}}}}{\hbar}e^{i\mathbf{k}\cdot\mathbf{x_m}} + B_m(\omega)\Omega, \tag{11}$$

$$(\omega - \omega_3 + i\epsilon)B_m(\omega) = \sum_{\mathbf{k}'} P_{\mathbf{k}'}^-(\omega)\frac{V_{BP_{\mathbf{k}'}}}{\hbar}e^{i\mathbf{k}'\cdot\mathbf{x_m}} + A_m(\omega)\Omega^*, \tag{12}$$

where the factors $e^{\pm i\mathbf{k}\cdot\mathbf{x_m}}$, $m=1$ to N, take into account the phase according to the position where the photon absorption (+) or emission (−) takes place. The interaction matrix elements $V_{\pm}$ are now relabelled as V_{ij}, to emphasize their correspondence with the transition from state $|i\rangle$ to state $|j\rangle$.

The interpretation of the above equations is straightforward. For example, Eq. (9) describes the production of a photon having wave number $\mathbf{k}$ and σ^+ polarization. The first term on the right-hand side states that this can occur through the emission of such a photon by the source. The second term says that this can also occur by the emission by any of the absorber nuclei, at positions $\mathbf{x}_m$, that were in the excited state $|2\rangle$. Equation (12) describes how nucleus m can reach the excited state $|3\rangle$. This is possible by the absorption of a σ^- photon, described by $P_{\mathbf{k}}^-(\omega)$, or by a transition from the excited state $|2\rangle$ in the same nucleus, described by $A_m(\omega)$. The other equations can be interpreted in a similar way.

D. Solving the equations

1. Solving for $S(\omega)$

Let us first try to find a solution for the source amplitude $S(\omega)$. After substitution of Eq. (9) into Eq. (8), we have

$$(\omega - \omega_s + i\epsilon)S(\omega) = 1 + S(\omega)\sum_{\mathbf{k}}\frac{|V_{SP_{\mathbf{k}}}|^2}{\hbar^2}\frac{1}{\omega - \omega_k + i\epsilon} + \sum_m A_m(\omega)\sum_{\mathbf{k}}\frac{V_{P_{\mathbf{k}}A}V_{SP_{\mathbf{k}}}}{\hbar^2}\frac{e^{-i\mathbf{k}\cdot\mathbf{x_m}}}{\omega - \omega_k + i\epsilon}. \tag{13}$$

The summation over $\mathbf{k}$ is transformed into an integral through the prescription[17]

$$\sum_{\mathbf{k}} \rightarrow \frac{V}{(2\pi)^3} \int d^3\mathbf{k}. \tag{14}$$

The sums over $\mathbf{k}$ of Eq. (13), which are now converted to integrals, can be evaluated using the relation[6]

$$\lim_{\epsilon \to 0^+} \frac{1}{x - a \pm i\epsilon} = P\left(\frac{1}{x-a}\right) \mp i\pi\delta(x-a), \tag{15}$$

where P indicates the principal part of an integral. For the second term on the right-hand side of Eq. (13) the principal part value gives rise to an energy shift, which can be incorporated into ω_s, while the δ function results in an imaginary term that is identified as a (partial radiative) linewidth of the source excited state,

$$\gamma_s^r = \frac{V}{(2\pi\hbar)^2} \int d^3\mathbf{k} |V_{SP_k}|^2 \delta(\omega - \omega_k). \tag{16}$$

It is straightforward to verify that all other (incoherent) decay channels of the source excited state, e.g, electron conversion, contribute in a similar way. Eventually, the total decay rate γ_s should correspond to the inverse of the lifetime of the source excited state.

The third term on the right-hand side of Eq. (13) describes a higher-order contribution with rapidly oscillating factors that will be neglected. This term describes the probability of reexcitation of the source nucleus by a photon coming back from the absorber, expressed by the sum over $A_m(\omega)$. Such a process is negligible because, in most cases, the solid angle subtended by the source is very small with respect to the absorber. In fact, this is the same as assuming that the source nucleus will decay in the same manner as it would if the absorber were absent.[7] The source term can, therefore, be approximated by

$$S(\omega) \approx \frac{1}{\omega - \omega_s + i\frac{\gamma_s}{2}}, \tag{17}$$

where the limit $\epsilon \rightarrow 0^+$ is taken.

2. Solution of $A_m(\omega)$ and $B_m(\omega)$

Solving Eq. (9) for $P_k^+(\omega)$ and substituting into Eq. (11) and solving Eq. (10) for $P_{k'}^-(\omega)$ and substituting into Eq. (12) gives the following set of coupled linear equations:

$$\begin{aligned}(\omega - \omega_2 + i\epsilon)A_m(\omega) &= \Omega B_m(\omega) + \sum_{\mathbf{k}} \frac{V_{AP_\mathbf{k}} V_{P_\mathbf{k}S} e^{i\mathbf{k}\cdot\mathbf{x_m}}}{\hbar^2(\omega - \omega_k + i\epsilon)\left(\omega - \omega_s + i\frac{\gamma_s}{2}\right)} \\ &+ \sum_{m'} A_{m'}(\omega) \sum_{\mathbf{k}} \frac{|V_{AP_\mathbf{k}}|^2}{\hbar^2} \frac{e^{-i\mathbf{k}\cdot(\mathbf{x_{m'}} - \mathbf{x_m})}}{\omega - \omega_k + i\epsilon},\end{aligned} \tag{18}$$

$$\begin{aligned}(\omega - \omega_3 + i\epsilon)B_m(\omega) &= \Omega^* A_m(\omega) + \sum_{m'} B_{m'}(\omega) \sum_{\mathbf{k}'} \frac{|V_{BP_{\mathbf{k}'}}|^2}{\hbar^2} \frac{e^{-i\mathbf{k}'\cdot(\mathbf{x_{m'}} - \mathbf{x_m})}}{(\omega - \omega_{k'} + i\epsilon)}.\end{aligned} \tag{19}$$

The sums over $\mathbf{k}$ and $\mathbf{k}'$ are evaluated in the same way as described above. Although the general model is formulated in three-dimensional space, we now restrict the calculations to the forward direction only. It can be argued that photons that reach the detector from a nonforward direction have experienced different optical paths and thus have different optical path lengths. Therefore, since we must sum over all coherent paths, destructive interference between the nonforward paths makes their contribution negligible. If only forward scattering is considered, all paths have the same optical path length and give a nonzero contribution to the radiation detected.

In this one dimension, the sum over m can be limited by assuming that an absorber nucleus m can only be excited by radiation coming from other nuclei m' that are located upstream ($x_{m'} < x_m$) and not by radiation scattered from nuclei downstream. In the first case all possible optical path lengths are the same and will add constructively, while in the latter they are not (see also Ref. 9 for a more quantitative treatment of this approximation). The terms with $m = m'$ yield the radiative decay $\gamma_{2/3}^r$ of the excited states and again, all other decay channels can be added to this decay leading to the total decay rate $\gamma_{2/3}$. The set of equations can then be rewritten as

$$\begin{aligned}\left(\omega - \omega_2 + i\frac{\gamma_2}{2}\right)A_m(\omega) &= \Omega B_m(\omega) - \frac{i\sqrt{\gamma_2^r}}{2}\left(\frac{V_{P_k S}}{\hbar}\right)\frac{e^{i(\omega/c)x_m}}{\left(\omega - \omega_s + i\frac{\gamma_s}{2}\right)} \\ &- \frac{i\gamma_2^r}{2}\sum_{m'=1}^{m-1} A_{m'}(\omega) e^{i(\omega/c)(x_m - x_{m'})},\end{aligned} \tag{20}$$

$$\begin{aligned}\left(\omega - \omega_3 + i\frac{\gamma_3}{2}\right)B_m(\omega) &= \Omega^* A_m(\omega) - \frac{i\gamma_3^r}{2}\sum_{m'=1}^{m-1} B_{m'}(\omega) e^{i(\omega/c)(x_m - x_{m'})},\end{aligned} \tag{21}$$

with γ_i^r the partial radiative decay rate from $|i\rangle$ to $|1\rangle$. Furthermore, we have defined

$$\sqrt{\gamma_2^r} \equiv \left(\frac{V_{P_k A}}{\hbar}\right)^{-1} \frac{V}{(2\pi\hbar)^2} \int d^3\mathbf{k} |V_{AP_k}|^2 \delta(\omega - \omega_k), \tag{22}$$

where it is assumed that $V_{P_k A}$ varies little around $\omega = \omega_k$. We now cast Eqs. (20) and (21) in a more symmetrical form by solving them for $A_m(\omega)$ and $B_m(\omega)$, but still expressing them as a function of $A_{m'}(\omega)$ and $B_{m'}(\omega)$,

$$A_m(\omega) = e^{i(\omega/c)x_m}\left[S^+(\omega) + \sum_{m'=1}^{m-1}\left(\frac{-i\gamma_2^r}{2}\right)\frac{\delta_3}{\delta_+\delta_-}A_{m'}(\omega)e^{-i(\omega/c)x_{m'}} + \sum_{m'=1}^{m-1}\left(\frac{\Omega}{\delta_2}\right)\left(\frac{-i\gamma_3^r}{2}\right)\frac{\delta_2}{\delta_+\delta_-}B_{m'}(\omega)e^{-i(\omega/c)x_{m'}}\right], \quad (23)$$

$$B_m(\omega) = e^{i(\omega/c)x_m}\left[\left(\frac{\Omega^*}{\delta_3}\right)S^+(\omega) + \sum_{m'=1}^{m-1}\left(\frac{-i\gamma_3^r}{2}\right)\frac{\delta_2}{\delta_+\delta_-}B_{m'}(\omega)e^{-i(\omega/c)x_{m'}} + \sum_{m'=1}^{m-1}\left(\frac{\Omega^*}{\delta_3}\right)\left(\frac{-i\gamma_2^r}{2}\right)\frac{\delta_3}{\delta_+\delta_-}A_{m'}(\omega)e^{-i(\omega/c)x_{m'}}\right], \quad (24)$$

with $S^+(\omega)$ defined in Eq. (26). We have adopted the shorthand notation $\delta_{s/2/3}=\omega-\omega_{s/2/3}+i\frac{\gamma_{s/2/3}}{2}$ and $\delta_\pm=\omega-\omega_\pm$, where we have introduced the two new frequencies $\omega_\pm$ according to

$$\omega_\pm = \frac{\left(\omega_2 - i\frac{\gamma_2}{2}\right)+\left(\omega_3 - i\frac{\gamma_3}{2}\right)}{2} \pm \sqrt{\left(\frac{\left(\omega_2 - i\frac{\gamma_2}{2}\right)-\left(\omega_3 - i\frac{\gamma_3}{2}\right)}{2}\right)^2 + |\Omega|^2}. \quad (25)$$

These frequencies arise due to the mixing interaction Ω and, hence, should be interpreted as the eigenfrequencies of the mixed levels.

For the moment, let us neglect the phase factor $e^i(\omega/c)x_m$ in Eqs. (23) and (24). They only give rise to an overall phase factor of the solution of A_m (and B_m) proportional to x_m. According to this set of equations, there are five ways to reach state $|2\rangle$ or state $|3\rangle$ in nucleus m, corresponding, respectively, with $A_m(\omega)$ and $B_m(\omega)$. These five paths can be divided into one source path $S^+(\omega)$, two intranuclear paths (transitions in nucleus m) and two extranuclear paths (transitions in different nuclei). It is obvious that every scattering process should include (and start with) the source path, which is given by the expression

$$S^+(\omega) \equiv \left(\frac{V_{P_kS}}{\hbar}\right)\left(\frac{-i\sqrt{\gamma_2^r}}{2}\right)\frac{\delta_3}{\delta_s\delta_+\delta_-}. \quad (26)$$

As we consider the incidence of a σ^+ photon, the source path always yields an excitation to state $|2\rangle$ (in any nucleus m).

The two intranuclear paths arise due to the mixing interaction and are schematically depicted in Fig. 3.

The two extranuclear paths are shown in Fig. 4 and represent the process of σ^+ (σ^-) emission in nucleus m' and absorption of this σ^+ (σ^-) photon by nucleus m, with $m' < m$.

FIG. 3. Pictographical representation of the two intranuclear paths along with their mathematical expression.

Now, to find a solution for $A_m(\omega)$ and $B_m(\omega)$, for arbitrary m, it is a question of counting. First, to reach state $|2\rangle$ or $|3\rangle$ in nucleus m, not all preceding nuclei must participate in the scattering process. If n nuclei are involved, then

$$A_m(\omega) = \sum_{n=0}^{m-1}\binom{m-1}{n}A_m^n(\omega), \quad (27)$$

where the binomial coefficient gives the number of ways n nuclei can be picked out of a set of $m-1$ nuclei. $A_m^n(\omega)$ describes the amplitude of state $|2\rangle$ in nucleus m, for the case where the photon has first been scattered by n preceding nuclei.

Each nucleus can interact in four possible ways, depending on the polarization state of the absorbed and emitted photon: $++$, $--$, $+-$, and $-+$, where the first sign corresponds to absorption and the second to emission. However, there are certain restrictions. If a nucleus has emitted a σ^+ photon, then the next nucleus must absorb this σ^+ photon, and, hence, this next nucleus has only two possible ways of interacting ($++$ and $+-$). Therefore, it is better not to consider all possible nuclear configurations, as they are not truly independent, but to consider the combination of emission in one nucleus and absorption in a following one. In Fig. 5 it is shown that these extranuclear combinations (or enc) can assume values of $+$ and $-$, independent of the preceding enc. They also coincide with the extranuclear paths identified in Fig. 4.

If there are $n+1$ absorber nuclei (n preceding+the last one) and if we apply the initial condition of a σ^+ incident photon and the final condition of arriving in state $|2\rangle$ (or $|3\rangle$), there are n enc. Thus, there are 2^n possible paths contributing to $A_m^n(\omega)$.

If there are p enc_+, then there should be $n-p$ enc_- processes. However, the number of *intranuclear* paths, corresponding to the number of *changes* in polarization, depends on how the p enc_+ are arranged between the $n-p$ enc_-. For example, for $n=5$ and $p=3$, the $+++--$ enc series yield a different number of intranuclear paths than the $+-+-+$

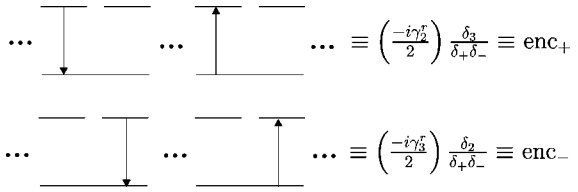

FIG. 4. Pictographical representation of the two extranuclear paths [or extranuclear combinations (enc)] along with their mathematical expression.

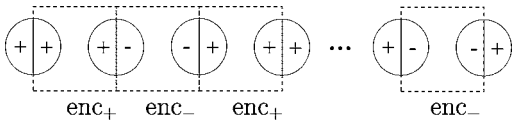

FIG. 5. Schematical representation of scattering of a σ^+ incident photon leading to the excitation of state $|2\rangle$ in nucleus m. Each nucleus that takes part in the process is depicted by a circle where the left half represents the absorption and the right half the emission process. The dashed squares represent the independent extranuclear combinations (see text).

enc series. It can be shown that, if k denotes the number of enc_+ enclosed by at least one enc_- (preceding and succeeding), then

$$\sum_{k=0}^{p}\binom{n-p-1}{k}\left(\frac{|\Omega|^2}{\delta_2\delta_3}\right)^{k+1}\sum_{l=0}^{(p-k-1)}\binom{p-k-1}{l}\binom{k+2}{l+1}$$

for $A_m^n(\omega)$, and

$$\frac{\Omega^*}{\delta_3}\sum_{k=0}^{p}\binom{n-p}{k}\left(\frac{|\Omega|^2}{\delta_2\delta_3}\right)^{k}\sum_{l=0}^{(p-k-1)}\binom{p-k-1}{l}\binom{k+1}{l+1}$$

for $B_m^n(\omega)$ are the amplitudes of intranuclear paths belonging to each (n,p) pair. The sum over l accounts for the possible ways to arrange $(p-k)$ other enc_+ on $(k+2)$ [or $(k+1)$] places.

Finally, taking into account the above prescription, we can reconstruct the solutions

$$A_m(\omega)=\frac{-i\sqrt{\gamma_2^r}}{2}\left(\frac{V_{P_kS}}{\hbar}\right)\frac{\delta_3 e^{i(\omega/c)x_m}}{\delta_s\delta_+\delta_-}\left(1+\sum_{n=1}^{m-1}\binom{m-1}{n}\frac{1}{(\delta_+\delta_-)^n}\right.$$
$$\times\left\{\left(\frac{-i\gamma_2^r\delta_3}{2}\right)^n+\sum_{p=0}^{n-1}\left(\frac{-i\gamma_3^r\delta_2}{2}\right)^{n-p}\left(\frac{-i\gamma_2^r\delta_3}{2}\right)^p\right.$$
$$\times\left[\binom{n-p-1}{p}\left(\frac{|\Omega|^2}{\delta_2\delta_3}\right)^{p+1}+\sum_{k=0}^{p-1}\binom{n-p-1}{k}\right.$$
$$\left.\left.\left.\times\left(\frac{|\Omega|^2}{\delta_2\delta_3}\right)^{k+1}\sum_{l=0}^{(p-k-1)}\binom{p-k-1}{l}\binom{k+2}{l+1}\right]\right\}\right) \quad (28)$$

and

$$B_m(\omega)=\frac{-i\sqrt{\gamma_2^r}}{2}\left(\frac{V_{P_kS}}{\hbar}\right)\frac{\Omega^* e^{i(\omega/c)x_m}}{\delta_s\delta_+\delta_-}\left\{1+\sum_{n=1}^{m-1}\binom{m-1}{n}\frac{1}{(\delta_+\delta_-)^n}\right.$$
$$\times\sum_{p=0}^{n}\left(\frac{-i\gamma_3^r\delta_2}{2}\right)^{n-p}\left(\frac{-i\gamma_2^r\delta_3}{2}\right)^p\left[\binom{n-p}{p}\left(\frac{|\Omega|^2}{\delta_2\delta_3}\right)^p\right.$$
$$+\sum_{k=0}^{p-1}\binom{n-p}{k}\left(\frac{|\Omega|^2}{\delta_2\delta_3}\right)^{k}\sum_{l=0}^{(p-k-1)}\binom{p-k-1}{l}$$
$$\left.\left.\times\binom{k+1}{l+1}\right]\right\}, \quad (29)$$

where the phase factors are again explicitly included. The binomials in the above expressions of course vanish whenever the lower term exceeds the upper term.

3. Solution of the photon wave function

Let us first consider the σ^+ photon field. Substituting the expression for $S(\omega)$ and $A_m(\omega)$ into Eq. (9), we find an expression for $P_k^+(\omega)$,

$$P_k^+(\omega)=\left(\frac{V_{P_kS}}{\hbar}\right)\frac{1}{\delta_s(\omega-\omega_k+i\epsilon)}\left(1-\frac{i\gamma_2^r}{2}\sum_{m=1}^{N}P_{k,m}^+(\omega)\right) \quad (30)$$

with

$$P_{k,m}^+(\omega)=e^{i(x_m/c)(\omega-\omega_k)}\frac{\delta_3}{\delta_+\delta_-}\left(1+\sum_{n=1}^{m-1}\right.$$
$$\times\left\{\binom{m-1}{n}\frac{1}{(\delta_+\delta_-)^n}\left\{\left(\frac{-i\gamma_2^r\delta_3}{2}\right)^n\right.\right.$$
$$+\sum_{p=0}^{n-1}\left(\frac{-i\gamma_3^r\delta_2}{2}\right)^{n-p}\left(\frac{-i\gamma_2^r\delta_3}{2}\right)^p\left[\binom{n-p-1}{p}\right.$$
$$\times\left(\frac{|\Omega|^2}{\delta_2\delta_3}\right)^{p+1}+\sum_{k=0}^{p-1}\binom{n-p-1}{k}$$
$$\left.\left.\left.\times\left(\frac{|\Omega|^2}{\delta_2\delta_3}\right)^{k+1}\sum_{l=0}^{p-k-1}\binom{p-k-1}{l}\binom{k+2}{l+1}\right]\right\}\right) \quad (31)$$

The interpretation of $P_k^+(\omega)$ is straightforward. The first term is the amplitude of a photon k that is not scattered (the original σ^+ source photon), while the subsequent terms describe the amplitudes for scattering at position $x_1,x_2,\ldots,x_m$. The factor δ_s^{-1} will eventually lead to a convolution of the (frequency) spectrum of the photon field with the spectrum of the incident field, centered at ω_s.

According to Refs. 7–11, one can represent the (one-dimensional) radiation wave function $\psi(x,t)$ as an infinite sum of plane waves

$$\psi(x,t)=\sum_k\frac{e^{i(kx-\omega_k t)}}{\sqrt{L}}p_k(t)=\frac{\sqrt{L}}{2\pi c}\int_{-\infty}^{\infty}d\omega_k e^{-i\omega_k(t-x/c)}p_k(t) \quad (32)$$

with $p_k(t)$ the time-dependent (classical) amplitude of a plane wave with wave number k. We admit that this transition from the quantum to the classical domain is rather sudden and should be more thoroughly derived. In the appendix we will justify this suggestion for the photon wave function. For now, we take Eq. (32) for granted and continue the derivation of the wave function.

It is also possible to express $\psi(x,t)$ in frequency domain by a Fourier transformation of Eq. (32),

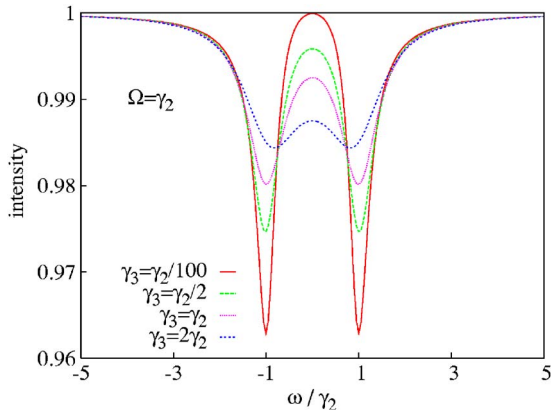

FIG. 6. (Color online) Simulation of the transmitted radiation in the thin absorber limit and for different values of γ_3 with a fixed mixing strength $\Omega=\gamma_2$.

$$\psi(x,\omega)=\int_{-\infty}^{\infty}dt\,\psi(x,t)e^{i\omega t} \tag{33}$$

$$=\frac{\sqrt{L}}{2\pi c}\int_{-\infty}^{\infty}d\omega_k e^{i\omega_k(x/c)}\underbrace{\int_{-\infty}^{\infty}dt p_k(t)e^{i(\omega-\omega_k)t}}_{=iP_k(\omega)}. \tag{34}$$

If we consider the ω_k-dependent terms of $P_k^+(\omega)$ in Eq. (30), then we distinguish the mth absorber term $[P_{k,m}^+(\omega)]$, which has a phase factor proportional to x_m, and a source term $[P_s(x,\omega)]$, without phase factor.[26] The calculation of the integral over ω_k is reduced to the integration of these ω_k-dependent terms,

$$\psi_s(x,\omega)\propto\int_{-\infty}^{\infty}d\omega_k\frac{e^{i\omega_k(x/c)}}{\omega-\omega_k+i\epsilon} \tag{35}$$

$$\propto 2\pi i e^{i\omega(x/c)}\theta(x)\quad\text{for }\epsilon\to 0^+ \tag{36}$$

and

$$\psi_{k,m}^+(x,\omega)\propto e^{i\omega(x_m/c)}\int_{-\infty}^{\infty}d\omega_k\frac{e^{i\omega_k[(x/c)-(x_m/c)]}}{\omega-\omega_k+i\epsilon} \tag{37}$$

$$\propto 2\pi i e^{i\omega(x/c)}\theta(x-x_m)\quad\text{for }\epsilon\to 0^+. \tag{38}$$

The appearance of the $\theta(x)$ Heaviside step function ensures a physical meaningful result. For the source term this means the detector position x should be downstream of the source (nucleus), located at $x=0$, whereas the mth absorber term only is relevant when this mth nucleus is in front of the detector.

The σ^+ photon wave function is now calculated as

$$\psi^+(x,\omega)=e^{i\omega(x/c)}\psi_s(\omega)\left[1+\sum_{n=0}^{N-1}\binom{N}{n+1}\psi_n^+(\omega)\right] \tag{39}$$

with the source term

$$\psi_s(\omega)=-\left(\frac{V_{P_kS}\sqrt{L}}{\hbar c}\right)\frac{1}{\delta_s} \tag{40}$$

and the absorber terms

$$\psi_n^+(\omega)=\frac{1}{(\delta_+\delta_-)^{n+1}}\left\{\left(\frac{-i\gamma_2^r\delta_3}{2}\right)^{n+1}+\sum_{p=0}^{n-1}\left(\frac{-i\gamma_3^r\delta_2}{2}\right)^{n-p}\left(\frac{-i\gamma_2^r\delta_3}{2}\right)^{p+1}\times\left[\binom{n-p-1}{p}\left(\frac{|\Omega^2|}{\delta_2\delta_3}\right)^{p+1}+\sum_{k=0}^{p-1}\binom{n-p-1}{k}\times\left(\frac{|\Omega^2|}{\delta_2\delta_3}\right)^{k+1}\sum_{l=0}^{p-k-1}\binom{p-k-1}{l}\binom{k+2}{l+1}\right]\right\}. \tag{41}$$

It is seen that, due to the reconstruction of the total wave packet, the dependence on the positions of the individual scattering centers disappears. Instead, the field amplitude gains a uniform phase factor, which only depends on the total path length x between its creation in the source and its destruction at the detector.

The derivation of the σ^- photon wave function is completely analogous. Eventually, we obtain the σ^- wave function

$$\psi^-(x,\omega)=e^{i\omega(x/c)}\psi_s(\omega)\sum_{n=0}^{N-1}\binom{N}{n+1}\psi_n^-(\omega) \tag{42}$$

with $\psi_s(\omega)$ defined in Eq. (40) and

$$\psi_n^-(\omega)=\left(\frac{-i\sqrt{\gamma_2^r\gamma_3^r}}{2}\right)\frac{\Omega^*}{(\delta_+\delta_-)^{n+1}}\left\{\sum_{p=0}^{n}\left(\frac{-i\gamma_3^r\delta_2}{2}\right)^{n-p}\left(\frac{-i\gamma_2^r\delta_3}{2}\right)^{p}\times\left[\binom{n-p}{p}\left(\frac{|\Omega^2|}{\delta_2\delta_3}\right)^{p}+\sum_{k=0}^{p-1}\binom{n-p}{k}\left(\frac{|\Omega^2|}{\delta_2\delta_3}\right)^{k}\times\sum_{l=0}^{p-k-1}\binom{p-k-1}{l}\binom{k+1}{l+1}\right]\right\}. \tag{43}$$

Except for the source term, the expression of the σ^- wave function bears a very close resemblance with the σ^+ wave function. So, once the photon has undergone one scattering, both fields develop in more or less the same way.

In the case without mixing interaction ($\Omega=0$), the photon fields reduce to

$$\psi^+(x,\omega)=e^{i\omega(x/c)}\psi_s(\omega)\left[1+\sum_{n=1}^{N}\binom{N}{n}\left(-\frac{i\gamma_2^r}{2}\frac{1}{\delta_2}\right)^n\right], \tag{44}$$

$$\psi^-(x,\omega)=0, \tag{45}$$

which is exactly the Fourier transform of the time-dependent photon wave function calculated by Hoy[8] in the case of scattering in a single-resonance nuclear medium [see Eq. (A24) in Ref. 8].

If the detector is not polarization sensitive, the measurable transmitted intensity in the case of a σ^+ source photon as a function of ω_s is given by

$$I(\omega_s) = \frac{1}{2\pi}\int_{-\infty}^{\infty} d\omega[|\psi^+(x,\omega)|^2 + |\psi^-(x,\omega)|^2], \quad (46)$$

which is the observable that can be obtained experimentally.

III. RESULTS AND DISCUSSION

A. Thin absorber limit

We start the discussion of Eq. (39) and Eq. (42) with the most simple case, i.e., a thin absorber or $N=1$. This corresponds to a system where multiple scattering effects are negligible. Also in the most common experiments where optical EIT is observed, i.e., in vapors, dynamical effects are not taken into account. This limiting case, therefore, presents an ideal opportunity to make a comparison between optical EIT (in an atomic Λ-scheme) and the nuclear level mixing induced transparency.

From Eq. (39) and Eq. (42) we obtain

$$\psi_1^+(x,\omega) = e^{i\omega(x/c)}\psi_s(\omega)\left[1 + \left(\frac{-i\gamma_2^r}{2}\right)\frac{\delta_3}{\delta_+\delta_-}\right], \quad (47)$$

$$\psi_1^-(x,\omega) = e^{i\omega(x/c)}\psi_s(\omega)\left(\frac{-i\sqrt{\gamma_2^r\gamma_3^r}}{2}\frac{\Omega^*}{\delta_+\delta_-}\right), \quad (48)$$

where all parameters have been defined in the preceding section. If we disregard the convolution with the source spectrum, then the transmitted intensity is given, to first order in γ_2^r, by

$$I(\omega) = 1 + 2\,\mathrm{Im}\left(\frac{\gamma_2^r}{2}\frac{\delta_3}{\delta_+\delta_-}\right). \quad (49)$$

This intensity of the transmitted radiation is simulated in Fig. 6 in the case of $\Omega=\gamma_2$ and for different values of γ_3.

A first interesting feature is the appearance of the two frequencies $\omega_\pm$ in the expression of the photon fields, as defined in Eq. (25) (now hidden in the notation of $\delta_\pm$). If $\omega_2=\omega_3$ and $\gamma_2=\gamma_3$, then $\omega_\pm=\omega_2\pm\Omega-i\gamma_2/2$. In this case the transmitted intensity also reduces to

$$I_1(\omega) = 1 - \frac{\gamma_2^r\gamma_2}{2}\left(\frac{1}{(\omega-\omega_2-\Omega)^2+\frac{\gamma_2^2}{4}} + \frac{1}{(\omega-\omega_2+\Omega)^2+\frac{\gamma_2^2}{4}}\right), \quad (50)$$

which is just a sum of two Lorentzian absorption lines, centered at ω_+ and ω_-, respectively. These frequencies can thus be identified as the eigenfrequencies of the new levels that arise from the mixing interaction. These are called *mixed levels* and are split by $2\,\Omega$.[18] It has been argued before,[3,19] that a model of EIT in terms of mixed levels (also called dressed states) is equivalent to a model that explicitly includes a mixing interaction in the bare levels, which is in agreement with this model.

Furthermore, Eq. (50) implies that, if $\gamma_2=\gamma_3$, no interference is present in the transmitted spectrum. This can be understood as follows. The transparency effect as known in optical EIT relies on the creation of a coherence between the states $|1\rangle$ and $|3\rangle$, i.e., the creation of a *dark state*.[20] Any decay of these levels, here γ_3, immediately implies the decay of this coherence. If the decoherence is as fast a process as the creation of the coherence (Ω), there is no way to obtain the destructive interference that is necessary for the appearance of a transparency window. This implies that, if $\gamma_2=\gamma_3$, any reduction in absorption at the center of the initial absorption line is solely due to the *Stark splitting* of the levels.

In Fig. 6 it is seen that, if $\gamma_3<\gamma_2$, the absorption at the center of the levels decreases with decreasing γ_3. This corresponds to a typical case of optical EIT, where level $|3\rangle$ is a stable or metastable state. However, if $\gamma_3>\gamma_2$ there is constructive interference in the absorption of the resonant radiation, giving rise to an *enhanced* absorption at the center of the levels. We can therefore conclude that, although at first sight the nuclear EIT scheme seems to show strong equivalence with the optical Λ-scheme, a thin-absorber-limit analysis reveals that the difference in relaxation rates leads to two really distinct pictures, i.e., with or without (destructive) interference.

B. Thick absorber

Another important difference with a common, vapor-based, optical EIT system is the large probability of more than one scattering process. On its path through a thick medium (crystal) the gamma photon will encounter many nuclei with which it can interact. Moreover, all scattering events are coherent because, like in every standard Mössbauer setup, only the forward scattered radiation is considered.

Simulations of the transmitted intensity for the cases $N=5$, 10, 20, 30, 50, and 80 are shown in Figs. 7–9, respectively. Each right-hand figure shows the individual contributions of the transmitted radiation that has changed polarization ($I^{+-}+I^{-+}$) and the radiation that has retained its polarization ($I^{++}+I^{--}$), while the left-hand figure shows the total spectrum. We have also included the case of a σ^- incident photon, which is no more than interchanging the label 2 with label 3 in the equations for a σ^+ incident source photon. Because we are considering the *nuclear* Λ-scheme, we set $\gamma_3=\gamma_2$. The partial radiative decay rates γ_2^r and γ_3^r are substituted with their real experimental values: $\gamma_2^r=|C_{12}|^2\gamma_r=\gamma_r/3$ and $\gamma_3^r=|C_{13}|^2\gamma_r=\gamma_r$, with C_{ij} the product of the Clebsch-Gordan coefficient and the rotation matrix element of the $|i\rangle-|j\rangle$ transition[14] and $\gamma_r\approx\gamma/10$ in ^{57}Fe. The maximal resonant absorption is limited to 30%, which corresponds to the experimental situation. It is seen that this maximum absorption is almost reached for $N=50$ and saturation clearly broadens the spectrum for $N=80$.

From these simulations the following observations can be drawn. First, the transparency effect of the mixing interaction reduces with increasing number of effective nuclei. For ex-

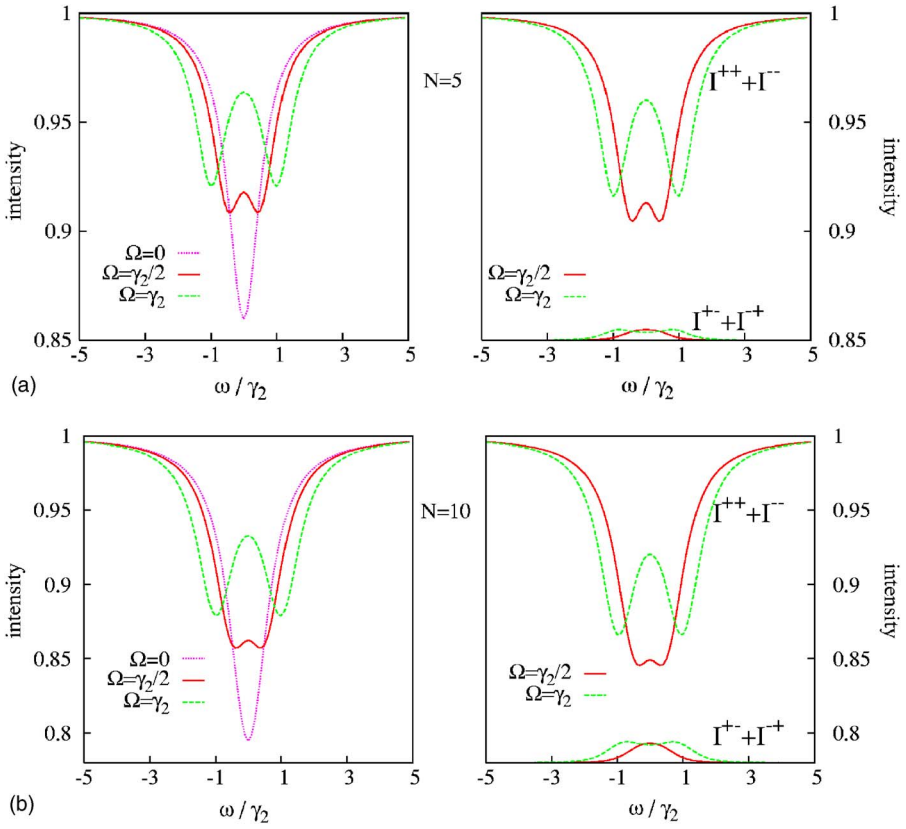

FIG. 7. (Color online) Simulated spectrum for $N=5$ (top) and $N=10$ (bottom) for different values of mixing interaction strength Ω. The right-hand figure shows the individual contributions of the transmitted radiation that has changed polarization (I^{+-}) and the radiation that has kept its polarization (I^{++}), while the left-hand figure shows the total transmitted radiation.

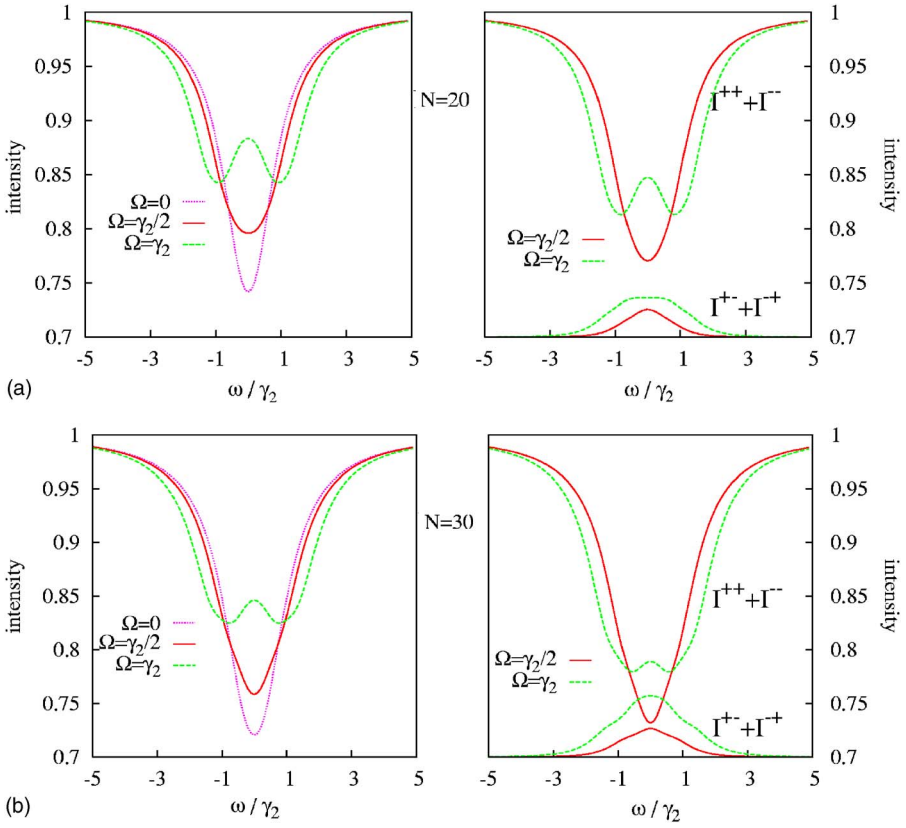

FIG. 8. (Color online) Simulated spectrum for $N=20$ (top) and $N=30$ (bottom) for different values of mixing interaction strength Ω. The right-hand figure shows the individual contributions of the transmitted radiation that has changed polarization (I^{+-}) and the radiation that has kept its polarization (I^{++}), while the left-hand figure shows the total transmitted radiation.

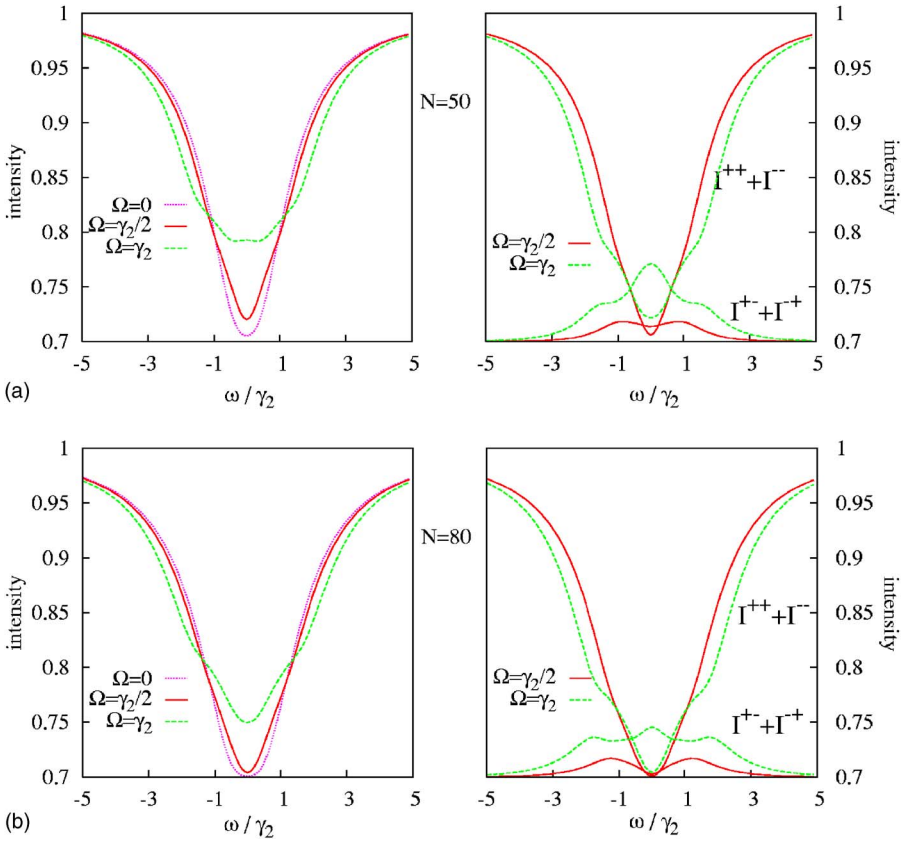

FIG. 9. (Color online) Simulated spectrum for $N=50$ (top) and $N=80$ (bottom) for different values of mixing interaction strength Ω. The right-hand figure shows the individual contributions of the transmitted radiation that has changed polarization (I^{+-}) and the radiation that has kept its polarization (I^{++}), while the left-hand figure shows the total transmitted radiation.

ample, for $N=5$, a mixing interaction of $\Omega=\gamma_2/2$ almost reduces the absorption at the line center with 50%, whereas the same mixing field has almost no observable effect any more for $N=80$.

We can also see a shift in the mechanism of the transparency. First, for small N, the main reason for the transparency is the Stark splitting of the excited states, which is best seen in the $I^{++}+I^{--}$ spectrum for $N=5$. For increasing N, however, the contribution of the $I^{+-}+I^{-+}$ part becomes more important, see also Fig. 10. It first reaches a maximum, at the line center, depending on Ω, and then shows a two-or three-peak structure. This two-peak structure (for $\Omega=\gamma_2/2$) also appears in the semiclassical Maxwell-Schrödinger model of nuclear resonant scattering in a Λ-scheme, see Ref. 21. But the three-peak structure has no semiclassical analogue. More simulations have shown that the center peak eventually disappears for large N, leaving behind a two-peak structure.

C. n-hop amplitudes

More insight in the multiple scattering construction of the final wave function is gained by simulating the different $\psi_n(\omega)$ terms of Eq. (41) [or Eq. (43)], *including the preceding binomial coefficient*. In Ref. 8 these $\psi_n(\omega)$ terms are referred to as the n-hop amplitudes,[27] because n is the number of nuclei with which the photon interacts, while hopping from one to the other. Simulations of the five first n-hop amplitudes for $N=20$ are shown in Fig. 11. The left-hand side of the figure gives the hop amplitudes for $\Omega=0$, expressed in Eq. (44), whereas the right-hand side shows the

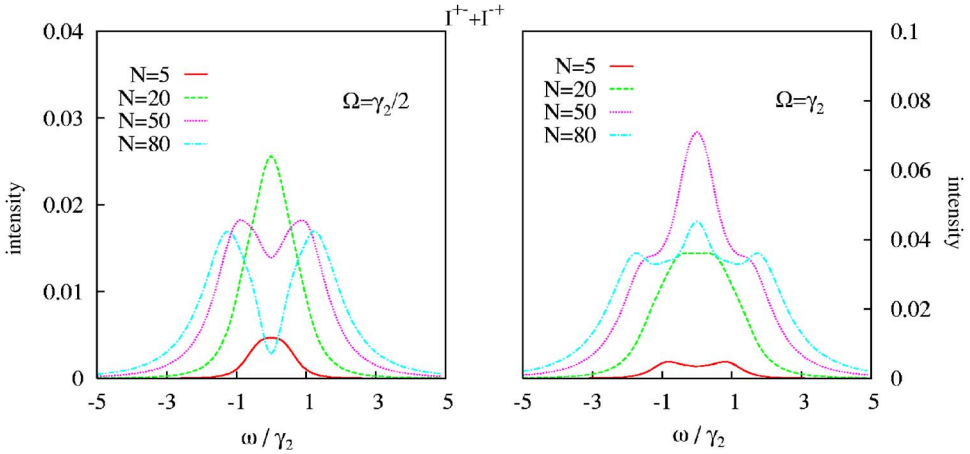

FIG. 10. (Color online) Simulated spectrum of the transmitted radiation that has changed polarization (I^{+-}) for different N and for $\Omega=\gamma_2/2$ (left-hand side) and $\Omega=\gamma_2$ (right-hand side).

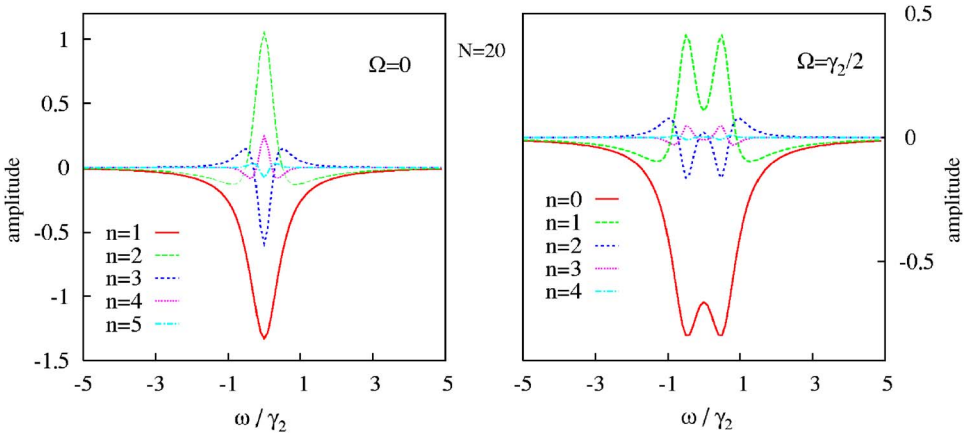

FIG. 11. (Color online) Simulation of the first n-hop amplitudes for $N=20$ with $\Omega=0$ (left-hand figure) and $\Omega=\gamma_2/2$ (right-hand figure).

$\psi_n^+(\omega)$ terms for $\Omega=\gamma_2/2$. It is clearly seen that the dominant first term yields a negative contribution, giving rise to the downward absorption peak in the Mössbauer transmission spectrum. This is the result of the π-phase shift[8] for single scattering at resonance. The second term (double scattering) yields a positive contribution, the third term again negative, and so on. For increasing n, however, this simple picture is seen to blur out, leading to an oscillating and rapidly decreasing net contribution.

The $\psi_n^+(\omega)$ terms in Fig. 11 show a highly decreasing peak amplitude for increasing n. It is worthwhile to go into more detail on this. For simplicity, let us take $\gamma_2'=\gamma_3'\equiv\gamma_r$. Then the strength (or peak amplitude at resonance) of each n is seen to be proportional to

$$\psi_n^+(\omega=\omega_0)\propto\binom{N}{n+1}\left(\frac{\gamma_r}{\gamma}\right)^{n+1}. \tag{51}$$

Because the condition that $\gamma_r<\gamma$ is always fulfilled, the second factor decreases exponentially for increasing n. The binomial coefficient, however, has a maximum for $n\approx N/2$. Hence, the significance of the contribution of an n-hop amplitude depends on the interplay between both terms. For example, the $(n=1)$-hop amplitude can gain a higher probability than the $(n=0)$-hop amplitude if the condition $N>1+(2\gamma_r/\gamma)$ is satisfied (e.g., if $\gamma_r/\gamma=0.1$ then $N>21$). Nevertheless, it is clear from Eq. (51) that terms with $n>N/2$ will always yield a very small contribution. Thus, at least one-half of the n-hop amplitudes can be neglected in the calculations. In Fig. 12 we illustrate this convergence of n-hop amplitudes by simulating the $I^{+-}+I^{-+}$ spectrum for $N=80$, including an increasing number of $\psi_n(\omega)$ terms. The solid line represents the full solution. It is seen that, already for $n=0$ to 12, the spectrum matches the full solution within the resolving power of the eye.

This information about the rapid convergence of the ψ_n series can drastically cut into the quite extensive computer time needed for simulations in the coherent path model.

D. Reduced transparency

This coherent path model also allows us to study the combined effect of different relaxation rates, γ_2 and γ_3, and multiple scattering in thick absorbers. Now, let us again consider the cases of $N=5$ and $N=20$. In Fig. 13 the total transmitted radiation is shown for $\Omega=\gamma_2/2$ and different values of γ_3, in the case of a σ^+ incident source photon. Comparing the spectra for $N=5$ with those for $N=20$, it is seen that the multiple scattering process destroys the transparency window. This can be understood as follows: even in a perfect EIT nucleus ($\gamma_3\ll\gamma_2$) an incident photon will always show a little absorption from its wings. In the scattering process with the next perfect EIT nucleus there is again a little absorption. Eventually, the absorption profile will show a considerable absorption even in the frequency region where there is only negligible absorption in the single scattering event. Hence, the effect of a decreasing transparency with increasing thickness is understood as a plain saturation effect.

E. Time-dependent properties

1. Photon wave function in time domain

In Sec. II D 3 an expression for the time-dependent photon wave function $\psi(x,t)$ is presented [Eq. (32)]. It is instructive to first consider the case when there is only a (decaying) source nucleus, as in the appendix. The expression for $p_k(t)$ is then given by Eq. (A6). Substituting its one-dimensional form in Eq. (32) yields

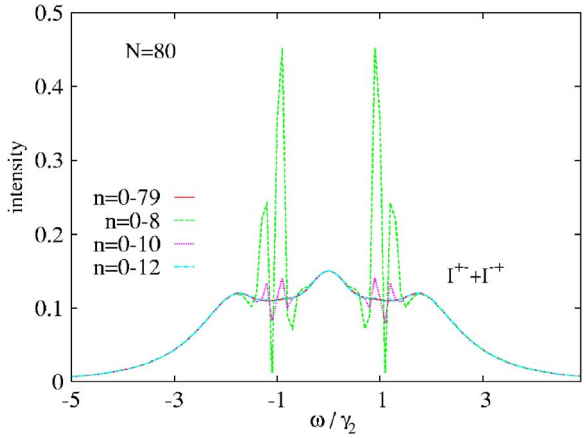

FIG. 12. (Color online) Simulation of the $I^{+-}+I^{-+}$ spectrum for $N=80$, including an increasing number of $\psi_n(\omega)$ terms. The solid line represents the full solution.

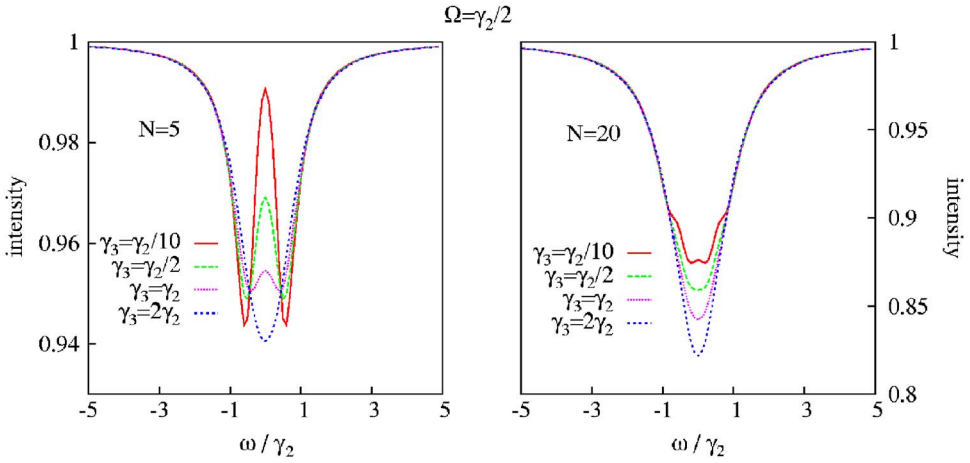

FIG. 13. (Color online) Simulation of the transmitted radiation in the case of $\Omega=\gamma_2/2$ for different values of γ_3, for $N=5$ (left-hand figure) and for $N=20$ (right-hand figure).

$$\psi(x,t) = \frac{\sqrt{L}}{2\pi c}\left(\frac{V_{P_k S}}{\hbar}\right)\int_{-\infty}^{\infty} d\omega_k e^{-i\omega_k\{t-(x/c)+(x_0/c)\}}\frac{1-e^{it(\omega_k-\omega_0+i\gamma_s/2)}}{\omega_k-\omega_s+i\gamma_s/2}. \quad (52)$$

The integral can be solved by conversion to complex coordinates and applying the theory of residues for complex closed loop integrals. The integral of the second term is nonzero for $\left(\frac{x}{c}-\frac{x_0}{c}\right)<0$, i.e., for radiation from the source emitted in the opposite direction of the detector. Hence, only the first term gives a physical contribution,

$$\psi(x,t) = -\frac{i\sqrt{L}}{c}\left(\frac{V_{P_k S}}{\hbar}\right)e^{-i\{t-[(x/c)-(x_0/c)]\}(\omega_s-i\gamma_s/2)}\theta\left[t-\left(\frac{x}{c}-\frac{x_0}{c}\right)\right]. \quad (53)$$

The appearance of the Heaviside step function ensures that the signal emitted by the source nucleus does not travel faster than the speed of light in vacuum.

Equation (53) is very similar to the photon wave function obtained in, Ref. 22, except for a $|\mathbf{r}-\mathbf{r}_0|^{-1}$ dependence. The intensity of radiation emitted from a point source into 4π should indeed decrease according to $|\mathbf{r}-\mathbf{r}_0|^{-2}$. The reason why we do not obtain this factor is simply because our approach is one-dimensional. In one dimension the energy of the field is not distributed over an ever increasing spherical surface, but instead, propagates undiminished in the one-dimensional space. In our case, all photons emitted by the point source have traveled more or less the same distance before detection. Hence, the $|\mathbf{r}-\mathbf{r}_0|^{-1}$ factor yields no more than an overall reduction of intensity.

Let us now turn to the case with an absorber consisting of N effective nuclei. To find an expression for $p_k(t)$, we make a Fourier transformation to time domain of $P_k(\omega)$ [Eq. (30)]. We only deal with poles with negative imaginary part, which means that only for $t\geqslant 0$ the integral is nonzero. The physical meaning is obvious.

The calculations are simplified as it turns out that only the pole $\omega=\omega_k-i\epsilon$ will contribute to the final expression of $\psi(x,t)$. When integrated over ω_k all other poles only give a contribution if $x\leqslant x_m$, i.e., a nonphysical situation in which the detector (at position x) would be positioned in front of the absorber nuclei instead of behind.

The integral over ω_k can again be calculated by applying the theory of residues. Eventually, one finds the expression for the σ^+ photon wave field at position $x(\geqslant x_N)$ and time t, parametrized by $t'=t-x/c$ with the condition that $t'\geqslant 0$, for N effective scattering nuclei,

$$\psi_N^+(t') = \psi_s(t')\left[1+\sum_{n=0}^{N-1}\sum_{p=0}^{n}\sum_{k=0}^{p}\sum_{l=0}^{p-k-1}\binom{N}{n+1}\binom{n-p-1}{k}\times\binom{p-k-1}{l}\binom{k+2}{l+1}\times\left(\frac{-i\gamma_3^r}{2}\right)^{n-p}\left(\frac{-i\gamma_2^r}{2}\right)^{p+1}(|\Omega|^2)^{k+1}\psi_{npk}^+(t')\right] \quad (54)$$

with

$$\psi_s(t') = \left(\frac{-i\sqrt{L}}{\hbar c}\frac{V_{P_k S}}{\hbar}\right)e^{-it'[\omega_s-i(\gamma_s/2)]} \quad (55)$$

and

$$\psi_{npk}^+(t') = \frac{\delta_{s3}^{p-k}\delta_{s2}^{n-p-k-1}}{\delta_{s+}^{n+1}\delta_{s-}^{n+1}}+\sum_{i=0}^{n}\sum_{q=0}^{i}\sum_{r=0}^{q}\binom{n-p-k-1}{q-r}\times\binom{i-q+n}{i-q}\times\binom{p-k}{r}\times(-1)^{n-q}\left(\frac{\delta_{+3}^{p-k-r}\delta_{+2}^{n-p-k-1-q+r}}{\delta_{+s}^{n-i+1}\delta_{+-}^{n+i-q+1}}e^{-it'\delta_{+s}}\sum_{j=0}^{n-i}\frac{(it'\delta_{+s})^j}{j!}+\frac{\delta_{-3}^{p-k-r}\delta_{-2}^{n-p-k-1-q+r}}{\delta_{-s}^{n-i+1}\delta_{-+}^{n+i-q+1}}e^{-it'\delta_{-s}}\sum_{j=0}^{n-i}\frac{(it'\delta_{-s})^j}{j!}\right), \quad (56)$$

with $\delta_{ij}=\omega_i'-\omega_j'$ and $\omega_i'=\omega_i-i\gamma_i/2$. All parameters have been defined previously. In a similar way, one can calculate the σ^- photon wave field using the expression for $B_m(\omega)$ and Eq. (10). The general expression for the σ^- photon field is

$$\psi_N^-(t') = \psi_s(t')\frac{-i\sqrt{\gamma_2^r\gamma_3^r}}{2}\Omega^* \sum_{n=0}^{N-1}\sum_{p=0}^{n}\sum_{k=0}^{p}\sum_{l=0}^{p-k-1}\binom{N}{n+1}\binom{n-p}{k} \times \binom{p-k-1}{l}\binom{k+1}{l+1} \times \left(\frac{-i\gamma_3^r}{2}\right)^{n-p}\left(\frac{-i\gamma_2^r}{2}\right)^{p}(|\Omega|^2)^k\psi_{npk}^-(t') \quad (57)$$

with

$$\psi_{npk}^-(t') = \frac{\delta_{s3}^{p-k}\delta_{s2}^{n-p-k}}{\delta_{s+}^{n+1}\delta_{s-}^{n+1}} + \sum_{i=0}^{n}\sum_{q=0}^{i}\sum_{r=0}^{q}\binom{n-p-k}{q-r}\binom{i-q+n}{i-q} \times \binom{p-k}{r} \times(-1)^{n-q}\left(\frac{\delta_{+3}^{p-k-r}\delta_{+2}^{n-p-k-q+r}}{\delta_{+s}^{n-i+1}\delta_{+-}^{n+i-q+1}}e^{-it'\delta_{+s}}\sum_{j=0}^{n-i}\frac{(it'\delta_{+s})^j}{j!} + \frac{\delta_{-3}^{p-k-r}\delta_{-2}^{n-p-k-q+r}}{\delta_{-s}^{n-i+1}\delta_{-+}^{n+i-q+1}}e^{-it'\delta_{-s}}\sum_{j=0}^{n-i}\frac{(it'\delta_{-s})^j}{j!}\right). \quad (58)$$

As these amplitudes have mutually orthogonal polarizations, the total photon intensity that impinges on a detector at time t is given by

$$I(t) = |\psi^+(t)|^2 + |\psi^-(t)|^2 \quad (59)$$

$$\equiv I^{++} + I^{+-}, \quad (60)$$

for a σ^+ source photon.

2. Simulations

The easiest way to address these photon wave functions is through numerical simulations. It must be noted that the following simulations are only valid for the ideal case, i.e., there is no line broadening (except due to the finite lifetime), there are no neighboring absorption lines and all interaction is resonant ($f_r=1$).

In order to allow for a correct interpretation of the time-differential spectra in a three-level nuclear medium, we first consider the two-level system ($\Omega=0$) as a reference case. In Fig. 14 the total transmitted intensity for $N=50$ is plotted for different values of detuning $\delta=\omega_s-\omega_0$, with ω_s and ω_0 the frequency of the source photon and the nuclear transition, respectively. The other parameters involved are chosen as $\gamma_s=\gamma$ and $\gamma_r=\gamma/10$. In comparison with the bold solid line, which represents the normal lifetime curve (without absorber), there is a considerable speed-up effect at small times, i.e., the exponential has a steeper slope. It is followed by a dynamical beat. Both features are pure multiple scattering effects and have been discussed in detail in many papers, see, e.g., Refs. 5, 8, and 23–25.

If the incident radiation is detuned from resonance, the beating pattern shifts towards smaller times, while its amplitude increases. When $\delta \gtrsim 2\gamma$, it is seen that, for certain times, even more radiation is detected than without absorber.[28] Eventually, for large detuning, the spectrum approaches the normal lifetime curve, as is expected.

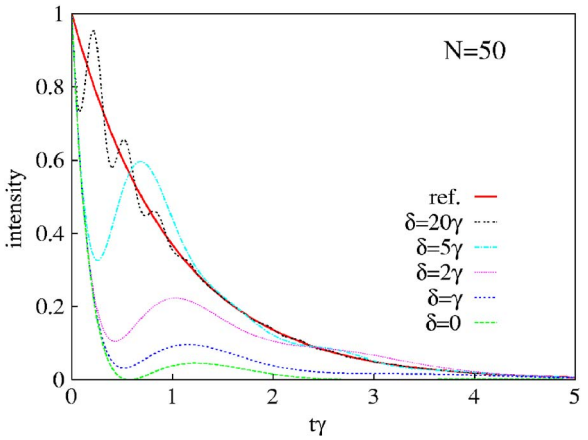

FIG. 14. (Color online) Simulated time-differential spectra in a two-level system ($\Omega=0$) for different values of $\delta=\omega_s-\omega_0$.

Figure 15 shows the simulations of the time-differential spectra in a nuclear three-level Λ system ($\Omega\neq 0$) for incidence of a σ^+ photon. Two absorbers ($N=5$ and $N=20$) and four different values of mixing interaction Ω are compared. We have chosen $\gamma_s=\gamma_3=\gamma_2$ and $\gamma_2^r=\gamma_3^r=\gamma_2/10$ and the incident radiation is tuned at the center of the (mixed) absorption lines, $\omega_s=\omega_2=\omega_3$. The bold solid line again represents the normal lifetime curve.

The speed-up and dynamical beat signatures are now less pronounced because the absorbers are chosen to be less thick. A feature for $\Omega\neq 0$ is the appearance of radiation with the orthogonal polarization state (I^{+-}). This radiation does not interfere with the incoming radiation and, hence, does not display the initial exponential decay curve (which originates from the decay of the source nucleus). It contributes to the total spectrum mainly at times several lifetimes later than $t=0$. This delay decreases, however, with increasing Ω, along with the amplitude of its contribution. For large Ω, the spectra tend to coincide with the normal lifetime curve, which could be compared with the case of a large detuning in the two-level system. For $N=5$ the effects are similar but less pronounced.

Simulations for the case of an optical Λ scheme (we choose $\gamma_3=\gamma_2/100$) are presented in Fig. 16. The spectra are very similar to the case with equal decay rates, except that the peak amplitude of the I^{+-} contribution is a little higher. Its shape and position have not changed.

From the solutions of the photon wave functions in the coherent path model we know that they are superpositions of n-hop amplitudes, with n (or $n+1$) the number of real scattering events. It is instructive to also visualize these n-hop amplitudes in their time-differential form. The first n-hop amplitudes for $N=20$ are shown in Fig. 17. As in the time-integrated picture, the first hop yields a negative contribution with respect to the (positive) exponential contribution of the noninteracting part of the radiation. This first hop amplitude decreases the transmitted intensity for small times, giving rise to the apparent speed-up effect. The contributions of the next n-hop amplitudes not only decrease, but also shift towards later times. It can be shown that, for $\Omega=0$, they reach their maximum strength exactly at $t_n=n(\gamma_2/2)^{-1}$. Hence,

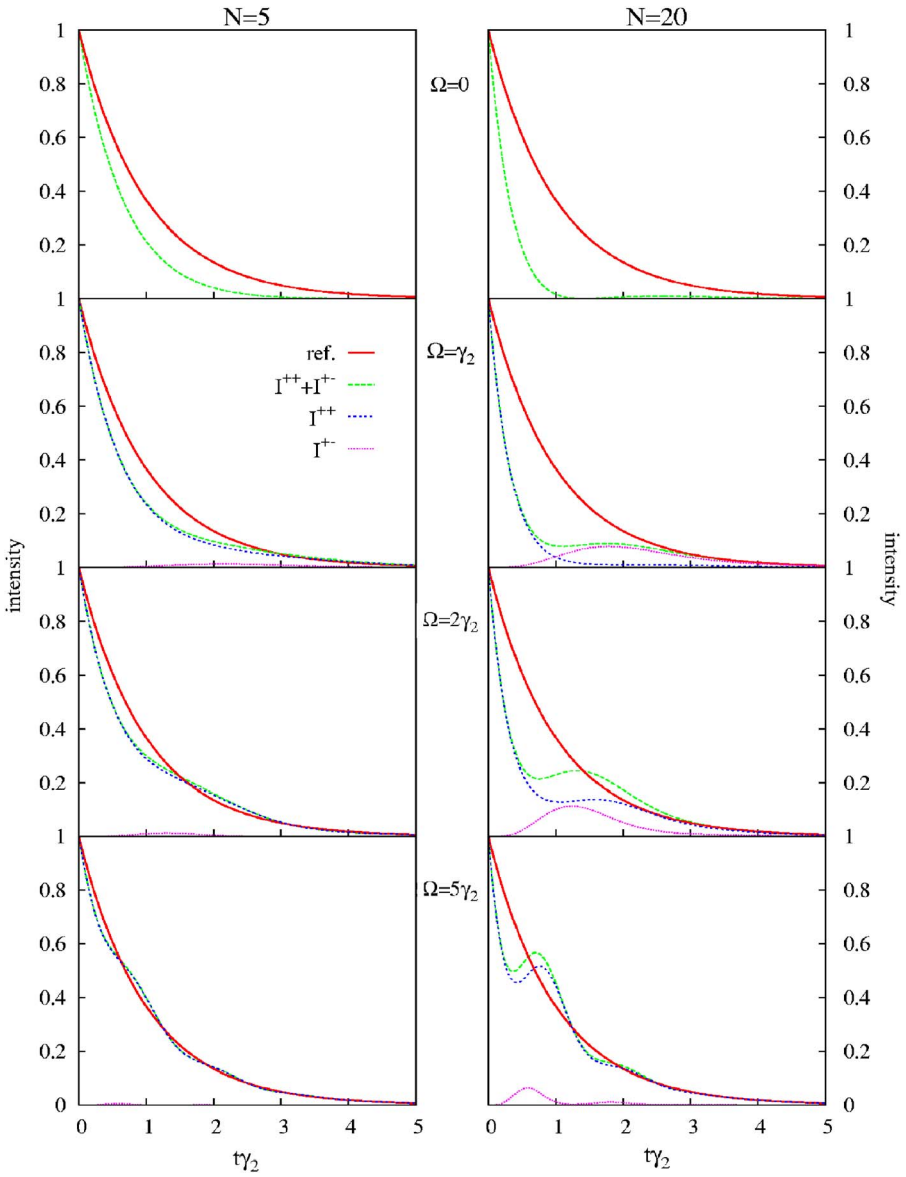

FIG. 15. (Color online) Simulated time-differential spectra in a three-level nuclear Λ system ($\gamma_3 = \gamma_2$) for different values of the mixing interaction Ω.

each n-hop amplitude is seen to be *delayed* with respect to the noninteracting radiation, which has its maximum transmission at $t=0$. The specific form of t_n supports the interpretation that the delay is simply due to the interaction of the radiation with the nuclear medium, where each interaction (scattering) adds $(\gamma_2/2)^{-1}$ to the delay. This also coincides with the intuitive picture that, upon absorption of the radiation, the nucleus decays with a lifetime of γ_2^{-1} and therefore slows down the radiation by the same factor.

For $\Omega = \gamma_2$, although the concept of a peak amplitude is less applicable, the contribution of an n-hop amplitude is also seen to shift towards later times with increasing n. Their oscillatory behavior, however, makes a straightforward interpretation more cumbersome. At least, we observe that the n-hop amplitudes for I^{+-} experience more delay than their I^{++} counterparts. The creation of the amplitudes belonging to I^{+-} involves at least one interaction with the mixing field. This interaction time is the reason for the additional delay.

IV. CONCLUSIONS

A fully quantum mechanical model for resonant scattering in a nuclear Λ-scheme is developed. The model allows a thorough analysis of both the close connection with optical EIT and the observed reduction of absorption in the $FeCO_3$ Mössbauer experiments.

It is shown that the level mixing or nuclear Λ-scheme is, in principle, equivalent with the Λ-schemes as widely investigated in quantum optics. However, in the nuclear case, the excited state is not coupled to a metastable state, which is of utmost importance for the creation of a dark state and hence EIT. If the two excited states have the same decay rate, any reduction in absorption at the line center can only stem from the nonresonance condition at the Stark split levels.

When multiple scattering is considered, a very interesting feature emerges from the equations. The breaking of the axial symmetry by a mixing interaction gives rise to the development of the complementary photon polarization state.

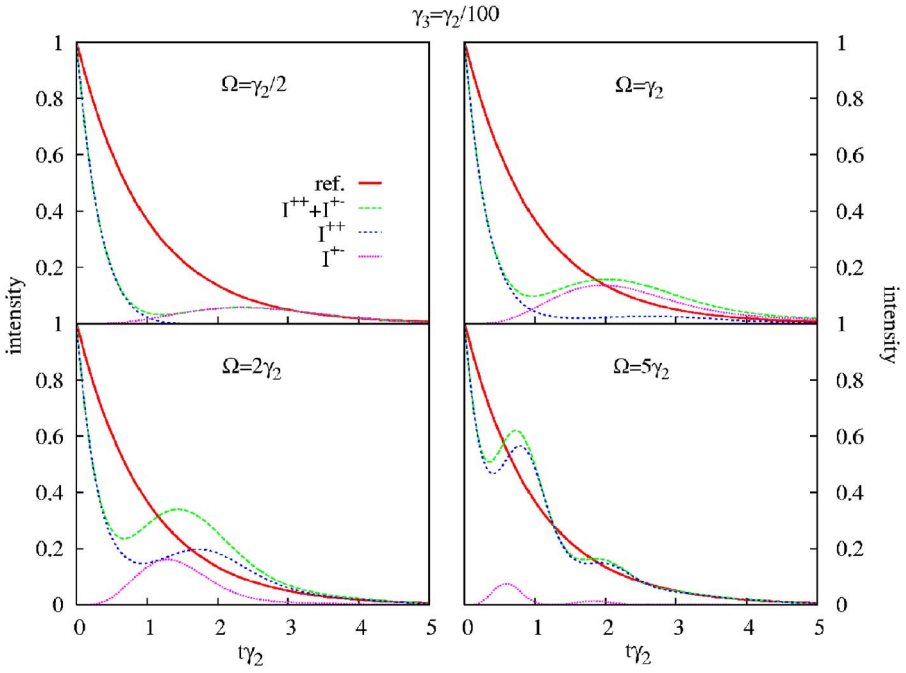

FIG. 16. (Color online) Simulated time-differential spectra in a three-level Λ system with $\gamma_3=\gamma_2/100$ and $N=20$, for different values of the mixing interaction Ω.

After the first scattering, an incident σ^+ photon can be transformed into a σ^- photon. At each subsequent scattering, the photon can flip its polarization state. It is shown that the complementary polarization state can be strongly enhanced by traveling through a thick medium, where the final photon field is a coherent sum over all possible quantum paths that have the same final polarization state. Due to its different polarization state this field does not interfere with the source field. This is translated to an apparent reduction of absorption. In a time domain picture this field can display a delay of several lifetimes with respect to a noninteracting field.

In conclusion, although the observable effects of transparency and delay of the gamma radiation in the nuclear Λ scheme studied are similar to EIT, they have a different source. They originate from a level mixing induced polarization change that is enhanced by multiple scattering.

ACKNOWLEDGMENTS

This work was supported by FWO-Vlaanderen and the IAP P5/07 program of the government of Belgium. One of the authors (S.G.) is a research assistant of FWO-Vlaanderen.

APPENDIX: THE PHOTON WAVE FUNCTION IN MORE DETAIL

The aim of this section is to justify the use of Eq. (32) as the photon wave function. We argue that, following Scully and Zubairy,[22] it is possible to assign a photon wave function status to the probability that a single photon will lead to the ejection of a photoelectron in a detector at point **r**. In resonance fluorescence experiments involving nuclei and gamma photons, the latter are commonly detected by means of a proportional counter. The detection principle is based on the ionization of (gas) atoms, which produces a detectable current. In this process the ionizing photon is destroyed. Therefore, the probability that a photon ionizes a detector atom at position **r** and between times t and $t+dt$ is proportional to $w(\mathbf{r},t)dt$ (Ref. 22) with

$$w(\mathbf{r},t) = |\langle \psi_f | E^{(+)}(\mathbf{r},t) | \psi_i \rangle|^2, \tag{A1}$$

where $|\psi_i\rangle$ and $|\psi_f\rangle$ are the initial and final state of the photon field. The photon is annihilated by the positive frequency part of the electric field operator

$$\mathbf{E}^{(+)}(\mathbf{r},t) = \sum_{\mathbf{k},\lambda} \mathcal{E}_{\mathbf{k}} \epsilon_{\mathbf{k}}^{\lambda} a_{\mathbf{k},\lambda} e^{i(\mathbf{k}\cdot\mathbf{r}-\omega_k t)}, \tag{A2}$$

where $\mathcal{E}_{\mathbf{k}}=(\hbar\omega_k/2\epsilon_0 V)^{1/2}$, $\epsilon_{\mathbf{k}}^{\lambda}$ a unit polarization vector, belonging to polarization state λ, and $a_{\mathbf{k},\lambda}$ the annihilation operator of a photon with wave vector **k** and polarization λ.

If $|\psi_i\rangle$ corresponds to a *single* photon state, designated by $|\psi_\gamma\rangle$, then $|\psi_f\rangle$ can only coincide with the vacuum state $|0\rangle$. Hence, the function

$$\psi(\mathbf{r},t) = \langle 0 | \mathbf{E}^{(+)}(\mathbf{r},t) | \psi_\gamma \rangle \tag{A3}$$

can be interpreted as a *single photon wave function*. It must be emphasized that in this approach the space and time dependent wave function only emerges from the photon interaction with a detector atom.

Let us now try to find an expression for this $|\psi_\gamma\rangle$ in the coherent path model. For simplicity, we only consider a source nucleus, and deal with the radiation it emits. Substituting the expression of the source amplitude $S(\omega)$ of Eq. (17) in Eq. (9) we find that

$$P_{\mathbf{k}}(\omega) = \left(\frac{V_{P_{\mathbf{k}}} S}{\hbar}\right) \frac{e^{-i\mathbf{k}\cdot\mathbf{r}_0}}{(\omega-\omega_k+i\epsilon)\left(\omega-\omega_s+i\frac{\gamma_s}{2}\right)}, \tag{A4}$$

where we have discarded the polarization dependence. Note that this equation is expressed in its three-dimensional form

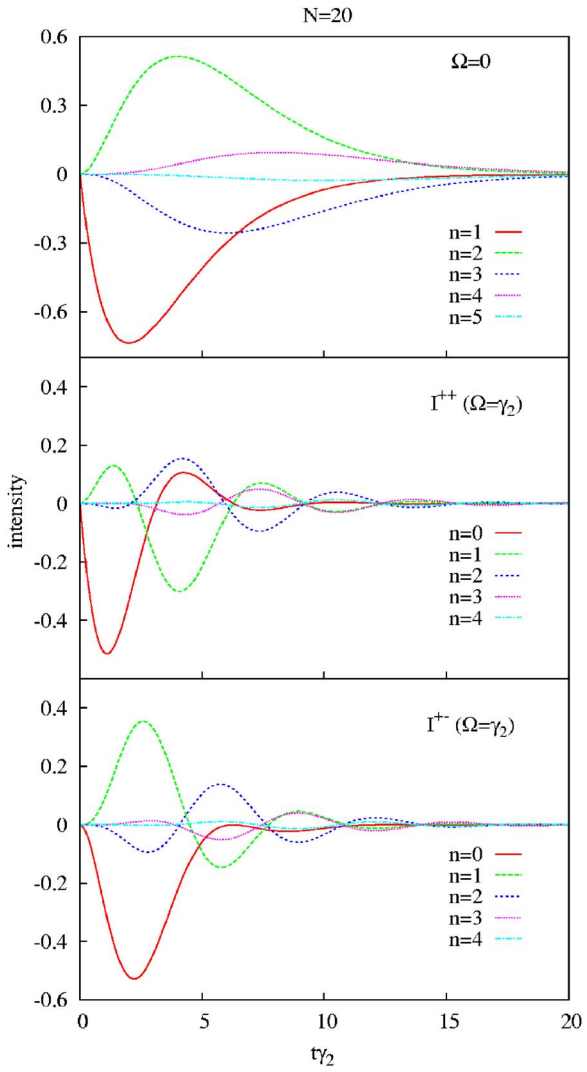

FIG. 17. (Color online) Simulations of the time-differential n-hop amplitudes in a two-level system (top figure) and in a three-level Λ-nuclear system (middle and bottom figure) with $\gamma_3 = \gamma_2$.

with $\mathbf{r_0}$ the position of the source nucleus. Applying the Fourier transform [Eq. (3)] back to time domain, we have

$$s(t) = e^{-\gamma_s t/2} \tag{A5}$$

and

$$p_{\mathbf{k}}(t) = \left(\frac{V_{P_{\mathbf{k}}S}}{\hbar}\right) e^{-i\mathbf{k}\cdot\mathbf{r}_0} \frac{1 - e^{it(\omega_k - \omega_s + i\gamma_s/2)}}{\omega_k - \omega_s + i\frac{\gamma_s}{2}}. \tag{A6}$$

According to Eq. (1), the state vector of this system can now be reconstructed as

$$|\Psi(t)\rangle = e^{-i\omega_s t} e^{-\gamma_s t/2} |S^e, \{0_{\mathbf{k}}\}\rangle + \sum_{\mathbf{k}} \left(\frac{V_{P_{\mathbf{k}}S}}{\hbar}\right) e^{-i\omega_k t} e^{-i\mathbf{k}\cdot\mathbf{r}_0} \frac{1 - e^{it(\omega_k - \omega_s + i\gamma_s/2)}}{\omega_k - \omega_s + i\frac{\gamma_s}{2}} |S^g, 1_{\mathbf{k}}\rangle. \tag{A7}$$

However, to stay consistent with the derivation of the photon wave function, resulting in the definition in Eq. (A3), we should express this state vector in an interaction representation. In this transition only the exponential factors corresponding to the eigenfrequencies of the states are omitted. The resulting expression now exactly equals Eq. (6.3.17) of Ref. 22, where the state vector of a decaying two-level atom is derived in a fully quantum mechanical way. Now, we can define the single-photon field state by taking the trace over the nuclear subsystem,

$$|\psi_\gamma(t)\rangle = \sum_{\mathbf{k}} p_{\mathbf{k}}(t) |1_{\mathbf{k}}\rangle \tag{A8}$$

$$= \sum_{\mathbf{k}} \left(\frac{V_{P_{\mathbf{k}}S}}{\hbar}\right) e^{-i\mathbf{k}\cdot\mathbf{r}_0} \frac{1 - e^{it(\omega_k - \omega_s + i\gamma_s/2)}}{\omega_k - \omega_s + i\frac{\gamma_s}{2}} |1_{\mathbf{k}}\rangle, \tag{A9}$$

which actually is a linear superposition of single-photon states with different wave vectors. Substituting this result and Eq. (A2) into Eq. (A3), we find

$$\psi(\mathbf{r}, t) = \sum_{\mathbf{k},\mathbf{k}'} \mathcal{E}_{\mathbf{k}'} \left(\frac{V_{P_{\mathbf{k}}S}}{\hbar}\right) e^{-i\omega_{k'} t} e^{i(\mathbf{k}'\cdot\mathbf{r} - \mathbf{k}\cdot\mathbf{r_0})} \times \frac{1 - e^{it(\omega_k - \omega_s + i\gamma_s/2)}}{\omega_k - \omega_s + i\frac{\gamma_s}{2}} \langle 0|a_{\mathbf{k}}|\psi_\gamma\rangle \tag{A10}$$

$$= \sum_{\mathbf{k}} \mathcal{E}_{\mathbf{k}} \left(\frac{V_{P_{\mathbf{k}}S}}{\hbar}\right) e^{-i\omega_k t} e^{i\mathbf{k}\cdot(\mathbf{r} - \mathbf{r_0})} \times \frac{1 - e^{it(\omega_k - \omega_s + i\gamma_s/2)}}{\omega_k - \omega_s + i\frac{\gamma_s}{2}} \tag{A11}$$

$$= \sum_{\mathbf{k}} \mathcal{E}_{\mathbf{k}} e^{i\mathbf{k}\cdot\mathbf{r} - i\omega_k t} p_{\mathbf{k}}(t). \tag{A12}$$

This last expression for the photon wave function equals the suggested expression in Eq. (32), except for the $\mathcal{E}_{\mathbf{k}}$ factor. Evaluating the sum over $\mathbf{k}$ in the Weisskopf-Wigner approximation, this term only yields an overall multiplication factor and can be neglected if one is only interested in relative magnitudes.

Therefore, we can state that, although the introduction of the photon wave function in Eq. (32) was only done in a heuristic way, its use for our purposes is now rigorously justified.

[1] M. Fleischhauer, A. Imamoglu, and J. P. Marangos, Rev. Mod. Phys. **77**, 633 (2005).
[2] R. Coussement, Y. Rostovtsev, J. Odeurs, G. Neyens, H. Muramatsu, S. Gheysen, R. Callens, K. Vyvey, G. Kozyreff, P. Mandel, R. Shakhmuratov, and O. Kocharovskaya, Phys. Rev. Lett. **89**, 107601 (2002).
[3] P. R. Berman, Phys. Rev. A **58**, 4886 (1998).
[4] S. Gheysen, R. Coussement, H. Muramatsu, R. N. Shakhmuratov, K. Vyvey, and J. Odeurs, J. Mod. Opt. **51**, 2589 (2004).
[5] F. J. Lynch, R. E. Holland, and M. Hamermesh, Phys. Rev. **120**, 513 (1960).
[6] W. Heitler, *The Quantum Theory of Radiation*, 3rd ed. (Oxford University Press, Oxford, 1954).
[7] S. Harris, Phys. Rev. **124**, 1178 (1961).
[8] G. R. Hoy, J. Phys.: Condens. Matter **9**, 8749 (1997).
[9] J. Odeurs, G. R. Hoy, C. L'abbé, R. N. Shakhmuratov, and R. Coussement, Phys. Rev. B **62**, 6148 (2000).
[10] G. R. Hoy and J. Odeurs, Phys. Rev. B **63**, 064301 (2001).
[11] G. R. Hoy, J. Odeurs, and R. Coussement, Phys. Rev. B **63**, 184435 (2001).
[12] W. C. McDermott and G. R. Hoy, Hyperfine Interact. **107**, 81 (1997).
[13] H. N. Ok, Phys. Rev. **185**, 472 (1969).
[14] M. Blume and O. C. Kistner, Phys. Rev. **171**, 417 (1968).
[15] A. Vértes, L. Korecz, and K. Burger, *Mössbauer Spectroscopy* (Elsevier, New York, 1979).
[16] I. I. Sobel'man, *Introduction to the Theory of Atomic Spectra* (Pergamon, Oxford, New York, 1972).
[17] R. Loudon, *The Quantum Theory of Light*, 2nd ed. (Clarendon, Oxford, New York, 1986).
[18] P. Put, R. Coussement, G. Scheveneels, F. Hardeman, I. Berkes, B. Hlimi, G. Marest, J. San, and E. H. Sayouty, Phys. Lett. **103A**, 151 (1984).
[19] R. Coussement, S. Gheysen, I. Serdons, R. Callens, K. Vyvey, R. N. Shakhmuratov, J. Odeurs, P. Mandel, Y. Rostovtsev, and O. Kocharovskaya, Hyperfine Interact. **151**, 93 (2003).
[20] K.-J. Boller, A. Imamoglu, and S. E. Harris, Phys. Rev. Lett. **66**, 2593 (1991).
[21] S. Gheysen and J. Odeurs (unpublished).
[22] M. O. Scully and S. Zubairy, *Quantum Optics* (Cambridge University Press, Cambridge, 1999).
[23] G. R. Hoy, Hyperfine Interact. **107**, 381 (1997).
[24] G. V. Smirnov, Hyperfine Interact. **123/124**, 31 (1999).
[25] U. van Bürck, Hyperfine Interact. **123/124**, 483 (1999).
[26] This is because we have chosen $x_0=0$.
[27] We must remark that, due to the specific form of our result, a $\psi_n^+(\omega)$ term corresponds to an $(n+1)$-hop (only in the right-hand figure).
[28] This is seen at times when the intensity curve crosses the normal lifetime curve. The overall, time-integrated intensity, however, is always smaller than in the case without absorber.